Heliyon 5 (2019) e01809

Contents lists available at ScienceDirect

Heliyon

journal homepage: www.heliyon.com

Synthesis, characterization and theoretical determination of corrosion inhibitor activities of some new 4,5-dihydro-1*H*-1,2,4-Triazol-5-one derivatives

Murat Beytur [a,*], Zeynep Turhan Irak [b], Sevda Manap [a], Haydar Yüksek [a]

[a] Kafkas University, Faculty of Science and Letters, Department of Chemistry, Kars, Turkey
[b] Igdir University, Engineering Faculty, Environmental Engineering Department, Igdir, Turkey

ARTICLE INFO

Keywords:
Organic chemistry
Theoretical chemistry
Corrosion inhibitory activity
1,2,4-Triazole-5-one
Quantum mechanical method
Electronic properties

ABSTRACT

Nine novel {bis-4-[(3-alkyl-5-oxo-1H-1,2,4-triazol-4(5H)-yl)-iminomethyl]-phenyl} [1,1′-biphenyl]-4,4′-disulfonates were synthesized and their structures were determined with spectral methods. Corrosion inhibitor activities of the title compounds were investigated using quantum mechanical methods. The parameters such as the Energy of the Highest Occupied Molecular Orbital (E_{HOMO}), Energy of the Lowest Unoccupied Molecular Orbital (E_{LUMO}), energy gap ($\Delta E = E_{LUMO} - E_{HOMO}$) and dipole moment (μ) which are related to the corrosion effectivity of the organic compounds whose the molecular geometry and electronic properties are especially studied, were determined by using the density function theory method. Using these calculation results, properties such as hardness (η), softness (σ), electronegativity (χ) values were calculated. Also quantum chemical parameters such as the fraction of transferred electrons (ΔN) between the iron surface and the 4,5-dihydro-1H-1,2,4-triazole-5-one derivative compounds were calculated. It has been discussed that which parameters have a good linear relationship with inhibition efficiency.

The results of the calculations show that there is a close relationship between the activity of organic-based corrosion inhibitors showing good corrosion inhibitor activity and the calculated quantum chemical parameters of the process. Thus, corrosion inhibitor activity can be predicted without conducting an experimental study.

1. Introduction

The field of study of heterocyclic molecules containing five member 1,2,4 triazole rings has been increasingly noted in recent years. A large number of researches were made for Schiff bases synthesized by Hugo Schiff for the first time in 1864 [1]. Structurally, in the first step, a carbonyl amine intermediate is formed from the condensation of the carbonyl group with the primary amine. In the second step, the Schiff base was formed at the end of the dehydration of this carbonyl amine intermediate compound [2]. Schiff bases have been extensively researched due to their application in many scientific and industrial fields [3, 4, 5, 6, 7]. Schiff base complexes have been observed to have different chemical activities showing reversible oxygen binding properties [8, 9], catalytic activities on olefins that getting hydrogenic [10], electrochemical electron transfer [11], photocromic features [12], and complexes formed by several toxic metals [13, 14].

It was determined that many organic compounds exhibit corrosion preventing (inhibitor) properties in corrosion studies, which is an important economic aspect. Organic inhibitors were found to prevent corrosion of the metal by adding a small amount to the medium. It is known that the inhibitory activities of organic inhibitors in cyclic structures containing heteroatom and conjugate bond, especially nitrogen, oxygen, phosphorus and sulfur are high [15]. The high formation of inhibitory activities of such compounds is due to the dissociated electron pairs and π electrons in their molecular structures. Schiff bases are considered great corrosion inhibitors because of the presence of electronegative nitrogen, oxygen, sulfur atoms, C=N group and aromatic ring in the molecular [16]. Presence of oxygen, nitrogen and sulfur in the structure of the sulfonates containing 4,5-dihydro-1H-1,2,4-triazole-5-one moieties increases likelihood of them being corrosion inhibitors.

Computational chemistry methods are as important as experimental methods in determining corrosion inhibitors. Without experiment, the activity of an inhibitor can be interpreted by using several quantum chemical parameters [17]. With quantum chemical calculations,

* Corresponding author.
E-mail address: muratbeytur@kafkas.edu.tr (M. Beytur).

https://doi.org/10.1016/j.heliyon.2019.e01809
Received 19 November 2018; Received in revised form 7 May 2019; Accepted 21 May 2019

compounds that can act as corrosion inhibitors between organic molecules can be designed. Quantum chemical parameters that are used frequently in the theoretical studies about corrosion can be grouped under the headings of atomic charges, molecular orbital energies, and energy [18]. In other words, it is necessary to calculate the parameters such as molecular activity, structure and load in corrosion inhibitors. Possible structure of the molecule can shed some light on the steric hindrance or how the inhibitor approaches the metal solution interface. In another approach, in orbital energies and the differences in orbital energies can also indicate how the inhibitor behaves electrochemically in the environment.

The ability of the inhibitor to react is attentively related the inhibitor's different parameters such as E_{HOMO}, E_{LUMO}, softness and hardness parameters obtained from E_{HOMO}, E_{LUMO} energies. Quantum chemical investigations were applied to find the corrosion inhibitory effect and molecular orbital energy levels of certain nitrogen containing heterocyclic organic compounds such as amides [19, 20], amino acids and hydroxy carboxylic acids [21], pyridine-pyrazole compounds [22], sulfonamides [23].

While in computational chemistry, molecules are calculated according to three basic methods ab initio, semi-experimental and molecular mechanics. The Density Function Theory (DFT) [24] is the method most commonly used by researchers in the last 20 years, which have been theorized by Hohenberg and Kohn. DFT is based on the principle that the total electron energy of a molecule is found based on the electron density of that molecule [25, 26]. The DFT method has been used to investigate the inhibitory activity of various corrosion inhibitors in different base sets [27, 28, 29, 30, 31, 32, 33].

2. Material and methods

Nine novel {bis-4-[(3-alkyl-5-oxo-1H-1,2,4-triazol-4(5H)-yl)-iminomethyl]-phenyl} [1,1′-biphenyl]-4,4′-disulfonates (M2-10) (Table 1) were obtained by treatment of 3-alkyl-4-amino-4,5-dihydro-1H-1,2,4-triazol-5-ones (T) with bis-(4-formylphenyl) [1,1′-biphenyl]-4,4′-disulfonate (A) (Scheme 1). The starting compounds T were synthesized according to literature [34]. The new synthesized molecules were clarified using spectral data (IR, ^{13}C-NMR, ^{1}H-NMR). The synthesized new molecules were theoretically evaluated for corrosion inhibitor activities.

2.1. Experimental methods

Synthesis section of this work was supported by the Scientific Research Projects Coordination Unit of Kafkas University (Project Number: 2016-FM-09).

Table 1
The name of 4,5-dihydro-1H-1,2,4-triazol-5-one derivatives and their abbreviations.

Abbr.	Compound Name
M1	{Bis-4-[4,5-dihydro-1*H*-1,2,4-triazole-5-on-4-yl)-azomethine]-phenyl} biphenyl-4, 4′disulfonate
M2	{Bis-4-[3-methyl-5-oxo-1H-1,2,4-triazol-4(5H)-yl)-iminomethyl]-phenyl} [1,1′-biphenyl]-4,4′-disulfonate
M3	{Bis-4-[3-ethyl-5-oxo-1H-1,2,4-triazol-4(5H)-yl)-iminomethyl]-phenyl} [1,1′-biphenyl]-4,4′-disulfonate
M4	{Bis-4-[3-*n*-propyl-5-oxo-1H-1,2,4-triazol-4(5H)-yl)-iminomethyl]-phenyl} [1,1′-biphenyl]-4,4′-disulfonate
M5	{Bis-4-[3-benzyl-5-oxo-1H-1,2,4-triazol-4(5H)-yl)-iminomethyl]-phenyl} [1,1′-biphenyl]-4,4′-disulfonate
M6	{Bis-4-[3-*p*-methylbenzyl-5-oxo-1H-1,2,4-triazol-4(5H)-yl)-iminomethyl]-phenyl} [1,1′-biphenyl]-4,4′-disulfonate
M7	{Bis-4-[3-*p*-methoxybenzyl-5-oxo-1H-1,2,4-triazol-4(5H)-yl)-iminomethyl]-phenyl} [1,1′-biphenyl]-4,4′-disulfonate
M8	{Bis-4-[3-*p*-chlorobenzyl-5-oxo-1H-1,2,4-triazol-4(5H)-yl)-iminomethyl]-phenyl} [1,1′-biphenyl]-4,4′-disulfonate
M9	{Bis-4-[3-*m*-chlorobenzyl-5-oxo-1H-1,2,4-triazol-4(5H)-yl)-iminomethyl]-phenyl} [1,1′-biphenyl]-4,4′-disulfonate
M10	{Bis-4-[3-phenyl-5-oxo-1H-1,2,4-triazol-4(5H)-yl)-iminomethyl]-phenyl} [1,1′-biphenyl]-4,4′-disulfonate

2.1.1. Used chemical and apparatus

The required chemical compounds were obtained from Aldrich and Merck AG. ^{1}H and ^{13}C NMR spectra, which used to elucidate the structures of the synthesized compounds, were obtained in DMSO-d_6 with TMS as internal standard by Bruker Ultrashield Plus Biospin spectrometer at 400 MHz and 100 MHz, respectively. Alpha-P Bruker FT-IR spectrometer were used IR spectra. Stuart SMP30 melting point apparatus were used in order to determine the melting points.

2.1.2. Synthesis

2.1.2.1. Procedure for the synthesis of bis-(4-formylphenyl) [1,1′-biphenyl]-4,4′-disulfonate (A). Biphenyl-4,4′-disulfonyl dichloride (10 mmol) was reacted with 4-hydroxybenzaldehyde (20 mmol) in ethyl acetate (100 mL). Then, triethylamine (0.02 mol) was slowly added in the solution at stirring at 0–5 °C with magnetic stirring. Stirring was continued for 2 h, and after that the mixture was refluxed for 3 hours and filtered. The crude product was crystallized several times in ethanol to afford compound **A**. Yield 92.69%. Mp: 114°C. IR (cm^{-1}): 3062 ($\upsilon_{C=CH}$), 2854 and 2791 (υ_{CHO}), 1699 ($\upsilon_{C=O}$), 1374 and 1168 (υ_{SO2}), 737 and 689 ($\upsilon_{1,4disubstituted\ benzenoid\ ring}$). ^{1}H NMR (400MHz, DMSO-d_6, δ): 7.32 (d, 4H, ArH; *J*=8.40 Hz), 7.94 (d, 4H, ArH; *J*=8.40 Hz), 8.01 (d, 4H, ArH; *J*=8.40 Hz), 8.06 (d, 4H, ArH; *J*=8.40 Hz), 9.93 (s, 1H, CHO), ^{13}C NMR (100MHz, DMSO-d_6, δ): 123.36 (4C); 126.82 (2C); 127.17 (2C); 128.42 (2C); 129.23 (2C); 129.52 (2C); 132.00 (4C); 134.56 (2C); 144.43 (2C); 149.40 (2C) (Ar-C), 192.39 (2C) (2CHO).

2.1.2.2. General procedure for the synthesis of compounds M2-9. Bis-(4-formylphenyl) [1,1′-biphenyl]-4,4′-disulfonate **A** (0.01 mol) was dissolved in acetic acid (15 mL) and reacted with the corresponding compound **T** (0.02 mol) to synthesize{bis-4-[(3-alkyl-5-oxo-1H-1,2,4-triazol-4(5H)-yl)-iminomethyl]-phenyl} [1,1′-biphenyl]-4,4′-disulfonates and was refluxed for 1.5 hour. Then, the solution evaporated at 50–55 °C *in vacuo*. The residue was crystallized several times in ethanol and pure **M2-9** compounds were obtained as colorless crystals.

2.1.2.2.1. {Bis-4-[3-methyl-5-oxo-1H-1,2,4-triazol-4(5H)-yl)-iminomethyl]-phenyl}[1,1′-biphenyl]-4,4′-disulfonate (M2). Yield 92.58%. Mp: 285ºC. IR (cm^{-1}): 3186 (υ_{NH}), 3062 ($\upsilon_{C=CH}$), 1699 ($\upsilon_{C=O}$), 1596 ($\upsilon_{C=N}$), 1376 and 1170 (υ_{SO2}), 744 and 690 ($\upsilon_{1,4disubstituted\ benzenoid\ ring}$). ^{1}H NMR (400MHz, DMSO-d_6, δ): 2.25 (s, 6H, $2CH_3$), 7.23 (d, 4H, ArH; *J*=8.80 Hz), 7.88 (d, 4H, ArH; *J*=8.80 Hz), 8.02 (d, 4H, ArH; *J*=8.40 Hz), 8.09 (d, 4H, ArH; *J*=8.80 Hz), 9.71 (s, 2H, 2N=CH), 11,85 (s, 2H, 2NH). ^{13}C NMR (100MHz, DMSO-d_6, δ): 11.01 ($2CH_3$), 122.71 (4C); 128.69 (4C); 129.05 (4C); 129.44 (4C); 132.86 (2C); 134.26 (2C); 143.93 (2C); 150.75 (2C) (Ar-C), 144.26 (2C) (2triazole C_3), 151.13 (2C) (2N=CH), 152.01 (2C) (2triazole C_5). Analysis: calcd. for $C_{32}H_{26}N_8O_8S_2$ (714.73): C, 53.78; H, 3.67; N, 15.68; S, 8.97 %, Found: C, 51.75; H, 3.62; N, 15.14; S, 10.59 %.

2.1.2.2.2. {Bis-4-[3-ethyl-5-oxo-1H-1,2,4-triazol-4(5H)-yl)-iminomethyl]-phenyl}[1,1′ biphenyl]-4,4′-disulfonate (M3). Yield 94.07%. Mp: 229ºC. IR (cm^{-1}): 3175 (υ_{NH}), 3073 ($\upsilon_{C=CH}$), 1695 ($\upsilon_{C=O}$), 1592 ($\upsilon_{C=N}$), 1374 and 1152 (υ_{SO2}), 741 and 691 ($\upsilon_{1,4disubstituted\ benzenoid\ ring}$). ^{1}H NMR (400MHz, DMSO-d_6, δ) 1.20 (t, 6H, $2CH_2\underline{CH_3}$; *J*=7.60 Hz), 2.66 (q, 4H, $2\underline{CH_2}CH_3$; *J*=7.20 Hz), 7.23 (d, 4H, ArH; *J*=8.40 Hz), 7.87 (d, 4H, ArH; *J*=7.20 Hz), 8.03 (d, 4H, ArH; *J*=8.40 Hz), 8.09 (d, 4H, ArH; *J*=8.40 Hz), 9.71 (s, 2H, 2N=CH), 11,87 (s, 2H, 2NH). ^{13}C NMR (100MHz, DMSO-d_6, δ): 10.03 ($2CH_2\underline{C}H_3$), 18.45 ($2\underline{C}H_2CH_3$), 122.74 (4C); 128.71 (4C); 129.06 (4C); 129.42 (4C); 132.89 (2C); 134.30 (2C); 143.94 (2C); 150.77 (2C) (Ar-C), 148.04 (2C) (2triazole C_3), 151.28 (2C) (2N=CH), 152.06 (2C) (2triazole C_5). Analysis: calcd. for $C_{34}H_{30}N_8O_8S_2$ (742.78): C, 54.98; H, 4.07; N, 15.10; S, 8.63 %, Found: C, 53.35; H, 3.99; N, 14.35; S, 10.53 %.

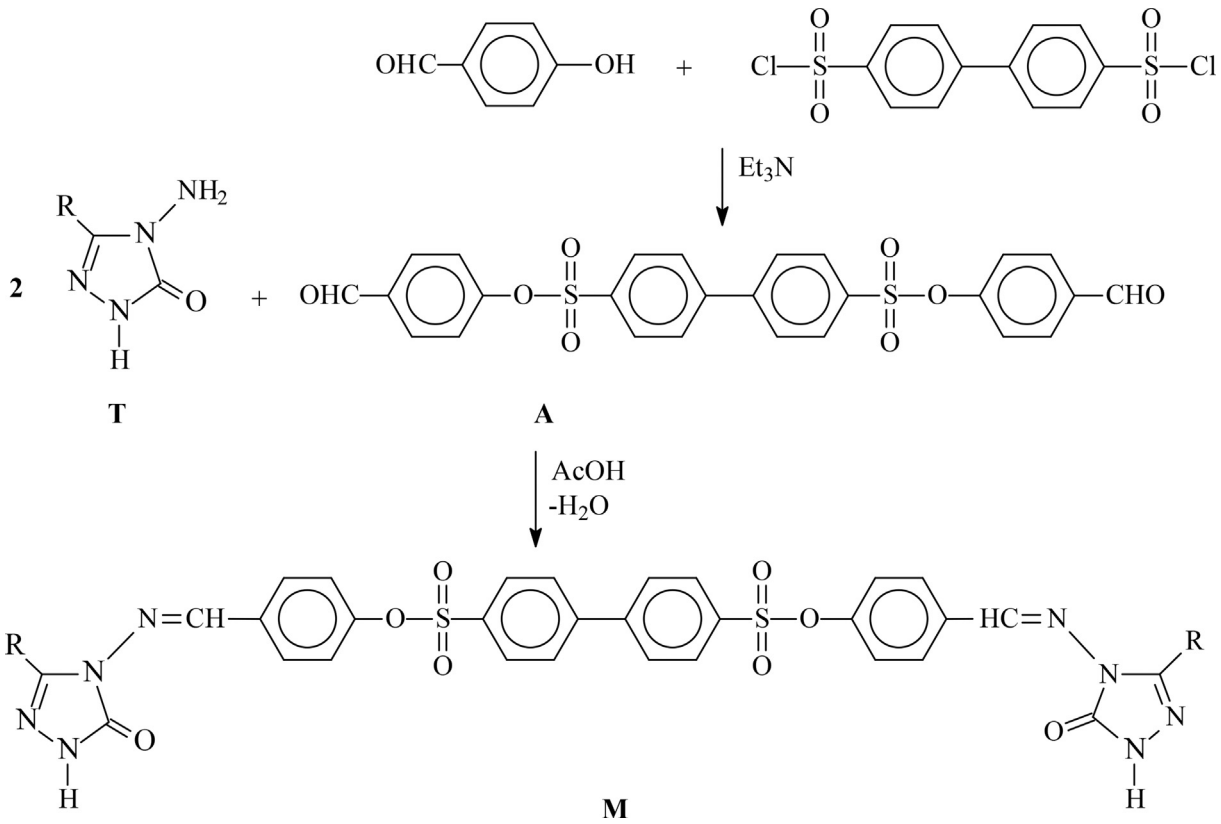

Scheme 1. Synthesis route of compounds M**(2-10)** M**2)** R = CH_3, **M3)** R = CH_2CH_3, **M4)** R = $CH_2CH_2CH_3$, **M5)** R = $CH_2C_6H_5$, **M6)** R = $CH_2C_6H_4CH_3$ (*p*-), **M7)** R = $CH_2C_6H_4OCH_3$ (*p*-), **M8)** R = $CH_2C_6H_4Cl$ (*p*-), **M9)** R = $CH_2C_6H_4Cl$ (*m*-), **M10)** R = C_6H_5.

2.1.2.2.3. {Bis-4-[3-n-propyl-5-oxo-1H-1,2,4-triazol-4(5H)-yl)-iminomethyl]-phenyl}[1,1′-biphenyl]-4,4′-disulfonate (M4). Yield 91.17%. Mp: 241ºC. IR (cm^{-1}): 3187 (υ_{NH}), 3075 ($\upsilon_{C=CH}$), 1694 ($\upsilon_{C=O}$), 1593 ($\upsilon_{C=N}$), 1379 and 1173 (υ_{SO2}), 735 and 694 ($\upsilon_{1,4disubstituted\ benzenoid\ ring}$). ^{1}H NMR (400MHz, DMSO-d_6, δ) 0.93 (t, 6H, $2CH_2CH_2CH_3$; *J*=7.20 Hz), 1.65 (sext, 4H, $2CH_2CH_2CH_3$; *J* = 7.60 Hz), 2.62 (t, 4H, $2CH_2CH_2CH_3$; *J* = 7.20 Hz), 7.23 (d, 4H, ArH; *J* = 8.80 Hz), 7.87 (d, 4H, ArH; *J* = 8.80 Hz), 8.03 (d, 4H, ArH; *J* = 8.80 Hz), 8.09 (d, 4H, ArH; *J* = 8.40 Hz), 9.71 (s, 2H, 2N = CH), 11,88 (s, 2H, 2NH). ^{13}C NMR (100MHz, DMSO-d_6, δ): 13.42 ($2CH_2CH_2CH_3$), 18.86 ($2CH_2CH_2CH_3$), 26.62 ($2CH_2CH_2CH_3$), 122.74 (4C); 128.70 (4C); 129.04 (4C); 129.40 (4C); 132.87 (2C); 134.29 (2C); 143.93 (2C); 150.76 (2C) (Ar-C), 146.88 (2C) (2triazole C_3), 151,21 (2C) (2N = CH), 152.07 (2C) (2triazole C_5). Analysis: calcd. for $C_{36}H_{34}N_8O_8S_2$ (770.83): C, 56.09; H, 4.45; N, 14.54; S, 8.32 %, Found: C, 55.24; H, 4.48; N, 13.27; S, 9.54 %.

2.1.2.2.4. {Bis-4-[3-benzyl-5-oxo-1H-1,2,4-triazol-4(5H)-yl)-iminomethyl]-phenyl}[1,1′-biphenyl]-4,4′-disulfonate (M5). Yield 89.54%. Mp: 258 °C. IR (cm^{-1}): 3181 (υ_{NH}), 3069 ($\upsilon_{C=CH}$), 1715 ($\upsilon_{C=O}$), 1592 ($\upsilon_{C=N}$), 1374 and 1174 (υ_{SO2}), 741 and 692 ($\upsilon_{1,4disubstituted\ benzenoid\ ring}$). ^{1}H NMR (400MHz, DMSO-d_6, δ) 4.03 (s, 4H, $2CH_2Ph$), 7.18-7.30 (m, 10H, ArH bonded to triazole C_3), 7.21 (d, 4H, ArH; *J* = 8.80 Hz), 7.81 (d, 4H, ArH; *J* = 8.80 Hz), 8.03 (d, 4H, ArH; *J* = 8.40 Hz), 8.09 (d, 4H, ArH; *J* = 8.40 Hz), 9.66 (s, 2H, 2N = CH), 12.00 (s, 2H, 2NH). ^{13}C NMR (100MHz, DMSO-d_6, δ) 30.98 (CH_2Ph), 122.71 (4C); 128.68 (4C); 129.08 (4C); 129.43 (4C); 132.81 (2C); 134.26 (2C); 143.92 (2C); 150.74 (2C) (Ar-C), 126.66 (2C); 128.40 (4C); 128.73 (4C); 135.70 (2C) (Ar-C bonded to triazole C_3), 146.18 (2C) (2triazole C_3), 151.10 (2C) (2N = CH), 151.82 (2C) (2triazole C_5). Analysis: calcd. for $C_{44}H_{34}N_8O_8S_2$ (866.92): C, 60.96; H, 3.95; N, 12.93; S, 7.40 %, Found: C, 59.49; H, 3.82; N, 12.39; S, 8.92 %.

2.1.2.2.5. {Bis-4-[3-p-methylbenzyl-5-oxo-1H-1,2,4-triazol-4(5H)-yl)-iminomethyl]-phenyl} [1,1′-biphenyl]-4,4′-disulfonate (M6). Yield 90.43%. Mp: 245 °C. IR (cm^{-1}): 3170 (υ_{NH}), 3065 ($\upsilon_{C=CH}$), 1705 ($\upsilon_{C=O}$), 1593 ($\upsilon_{C=N}$), 1374 and 1177 (υ_{SO2}), 745 and 696 ($\upsilon_{1,4disubstituted\ benzenoid\ ring}$). ^{1}H NMR (400MHz, DMSO-d_6, δ): 2.19 (s, 6H, 2*p*-$PhCH_3$), 3.96 (s, 4H, $2CH_2Ph$), 7.06 (d, 4H, ArH bonded to triazole C_3; *J*=7.60 Hz), 7.17 (d, 4H, ArH bonded to triazole C_3; *J*=8.00 Hz), 7.22 (d, 4H, ArH; *J* = 8.80 Hz), 7.82 (d, 4H, ArH; *J* = 8.80 Hz), 8.03 (d, 4H, ArH; *J* = 8.40 Hz), 8.09 (d, 4H, ArH; *J* = 8.40 Hz), 9.65 (s, 2H, 2N = CH), 11.99 (s, 2H, 2NH). ^{13}C NMR (100MHz, DMSO-d_6, δ): 20.53 (2*p*-$PhCH_3$), 30.59 ($2CH_2Ph$), 122.71 (4C); 128.67 (4C); 129.07 (4C); 129.42 (4C); 132.83 (2C); 134.27 (2C); 143.93 (2C); 150.74 (2C) (Ar-C), 128.59 (4C); 128.96 (4C); 132.58 (2C); 135.74 (2C) (Ar-C bonded to triazole C_3), 146.32 (2C) (2triazole C_3), 151.11 (2C) (2N = CH), 151.73 (2C) (2triazole C_5). Analysis: calcd. for $C_{46}H_{38}N_8O_8S_2$ (894.98): C, 61.73; H, 4.28; N, 12.52; S, 7.16 %, Found: C, 59.94; H, 4.11; N, 11.82; S, 8.89 %.

2.1.2.2.6. {Bis-4-[3-p-methoxybenzyl-5-oxo-1H-1,2,4-triazol-4(5H)-yl)-iminomethyl]-phenyl} [1,1′-biphenyl]-4,4′-disulfonate (M7). Yield 93.67%. Mp: 255 °C. IR (cm^{-1}): 3170 (υ_{NH}), 3063 ($\upsilon_{C=CH}$), 1706 ($\upsilon_{C=O}$), 1590 ($\upsilon_{C=N}$), 1372 and 1176 (υ_{SO2}), 747 and 698 ($\upsilon_{1,4disubstituted\ benzenoid\ ring}$). ^{1}H NMR (400MHz, DMSO-d_6, δ) 3.68 (s, 6H, $2OCH_3$), 3.95 (s, 4H, $2CH_2Ph$), 6.83 (d, 4H, ArH bonded to triazole C_3; *J*=8.40 Hz), 7.20 (d, 4H, ArH bonded to triazole C_3; *J*=8.80 Hz), 7.22 (d, 4H, ArH; *J* = 8.80 Hz), 7.84 (d, 4H, ArH; *J* = 8.80 Hz), 8.03 (d, 4H, ArH; *J* = 8.80 Hz), 8.09 (d, 4H, ArH; *J* = 8.80 Hz), 9.66 (s, 2H, 2N = CH), 11.98 (s, 2H, 2NH). ^{13}C NMR (100MHz, DMSO-d_6, δ) 30.13 (CH_2Ph), 54.97 (OCH_3), 122.72 (4C); 128.68 (4C); 129.07 (4C); 129.44 (4C); 132.84 (2C); 134.27 (2C); 143.93 (2C); 150.74 (2C) (Ar-C), 113.84 (4C); 126.39 (2C); 129.80 (4C); 158.06 (2C) (Ar-C bonded to triazole C_3), 146.49 (2C) (2triazole C_3), 151.12 (2C) (2N = CH), 151.79 (2C) (2triazole C_5). Analysis: calcd. for $C_{46}H_{38}N_8O_{10}S_2$ (926.98): C, 59.60; H, 4.13; N, 12.09; S, 6.92 %, Found: C, 58.04; H, 3.98; N, 11.37; S, 8.36 %.

2.1.2.2.7. {Bis-4-[3-p-chlorobenzyl-5-oxo-1H-1,2,4-triazol-4(5H)-yl)-iminomethyl]-phenyl} [1,1′-biphenyl]-4,4′-disulfonate (M8). Yield 92.38%. Mp: 250 °C. IR (cm^{-1}): 3190 (υ_{NH}), 3065 ($\upsilon_{C=CH}$), 1739, 1705 ($\upsilon_{C=O}$), 1596 ($\upsilon_{C=N}$), 1380 and 1174 (υ_{SO2}), 732 and 688 ($\upsilon_{1,4disubstituted\ benzenoid}$

ring). ^{1}H NMR (400MHz, DMSO-d_6, δ): 4.04 (s, 4H, 4CH_2Ph), 7.23 (d, 4H, ArH; J = 8.80 Hz), 7.33 (m, 8H, ArH bonded to triazole C_3), 7.83 (d, 4H, ArH; J = 8.80 Hz), 8.04 (d, 4H, ArH; J = 8.80 Hz), 8.10 (d, 4H, ArH; J = 8.80 Hz), 9.68 (s, 2H, 2N = CH), 12.05 (s, 2H, 2NH). ^{13}C NMR (100MHz, DMSO-d_6, δ) 30.33 (2CH_2Ph), 122.70 (4C); 128.66 (4C); 129.07 (4C); 129.45 (4C); 130.76 (4C); 132.76 (2C); 134.27 (2C); 143.93 (2C); 150.76 (2C) (Ar-C), 127.90 (4C); 128.33 (4C); 131.43 (4C); 134.65 (2C) (Ar-C bonded to triazole C_3), 145.83 (2C) (2triazole C_3), 151.09 (2C) (2N = CH), 151.85 (2C) (2triazole C_5). Analysis: calcd. for $C_{44}H_{32}N_8O_8S_2Cl_2$ (935.81): C, 56.47; H, 3.45; N, 11.97; S, 6.85 %, Found: C, 54.83; H, 3.33; N, 11.09; S, 8.42 %.

2.1.2.2.8. {Bis-4-[3-m-chlorobenzyl-5-oxo-1H-1,2,4-triazol-4(5H)-yl)-iminomethyl]-phenyl} [1,1′-biphenyl]-4,4′-disulfonate (M9). Yield 86.21%. Mp: 275 °C. IR (cm^{-1}): 3192 (υ_{NH}), 3071 ($\upsilon_{C=CH}$), 1700 ($\upsilon_{C=O}$), 1614, 1591 ($\upsilon_{C=N}$), 1375 and 1170 (υ_{SO2}), 748 and 684 ($\upsilon_{1,4disubstituted\ benzenoid\ ring}$). ^{1}H NMR (400MHz, DMSO-d_6, δ): 4.04 (s, 4H, 4CH_2Ph), 7.20 (d, 4H, ArH; J = 8.40 Hz), 7.22-7.32 (m, 6H, ArH bonded to triazole C_3), 7.38 (s, 2H, ArH bonded to triazole C_3), 7.81 (d, 4H, ArH; J = 8.80 Hz), 8.03 (d, 4H, ArH; J = 8.40 Hz), 8.09 (d, 4H, ArH; J = 8.80 Hz), 9.64 (s, 2H, 2N = CH), 12.03 (s, 2H, 2NH). ^{13}C NMR (100MHz, DMSO-d_6, δ): 30.61 (2CH_2Ph), 122.69 (4C); 126.71 (2C); 128.66 (4C); 129.10 (4C); 129.44 (2C); 132.78 (2C); 134.22 (2C); 143.91 (2C); 150.76 (2C) (Ar-C), 127.50 (2C); 128.91 (2C); 130.21 (2C); 131.43 (2C); 132.90 (2C); 138.07 (2C) (Ar-C bonded to triazole C_3), 145.66 (2C) (2triazole C_3), 151.06 (2C) (2N = CH), 151.81 (2C) (2triazole C_5). Analysis: calcd. for $C_{44}H_{32}N_8O_8S_2Cl_2$ (935.81): C, 56.47; H, 3.45; N, 11.97; S, 6.85 %, Found: C, 54.92; H, 1.41; N, 11.01; S, 18.45 %.

2.1.2.2.9. {Bis-4-[3-phenyl-5-oxo-1H-1,2,4-triazol-4(5H)-yl)-iminomethyl]-phenyl} [1,1′-biphenyl]-4,4′-disulfonate (M10). Yield 88.92%. Mp: 291 °C. IR (cm^{-1}): 3212 (υ_{NH}), 3096 ($\upsilon_{C=CH}$), 1701 ($\upsilon_{C=O}$), 1594 ($\upsilon_{C=N}$), 1378 and 1177 (υ_{SO2}), 741 and 686 ($\upsilon_{1,4disubstituted\ benzenoid\ ring}$). ^{1}H NMR (400MHz, DMSO-d_6, δ): 7.24 (d, 4H, ArH; J = 8.80 Hz), 7.50-7.52 (m, 6H, ArH bonded to triazole C_3), 7.84-7.88 (m, 4H, ArH bonded to triazole C_3), 7.84–7.88 (m, 4H, ArH), 8.02 (d, 4H, ArH; J = 8.40 Hz), 8.08 (d, 4H, ArH; J = 8.80 Hz), 9.67 (s, 2H, 2N = CH), 12.41 (s, 2H, 2NH). ^{13}C NMR (100MHz, DMSO-d_6, δ): 122.83 (4C); 128.72 (4C); 129.03 (4C); 129.67 (4C); 132.64 (2C); 134.27 (2C); 143.96 (2C); 150.92 (2C) (Ar-C), 126.70 (2C); 127.94 (4C); 128.51 (4C); 130.09 (2C) (Ar-C bonded to triazole C_3), 144.59 (2C) (2triazole C_3), 151.26 (2C) (2N = CH), 154.85 (2C) (2triazole C_5). Analysis: calcd. for $C_{24}H_{30}N_8O_8S_2$ (838.87): C, 60.14; H, 3.60; N, 13.36; S, 7.64 %, Found: C, 58.05; H, 3.51; N, 12.23; S, 9.17 %.

2.2. Calculation methods

The approximate geometry of the molecules in the gas phase and in the base case in three dimensions was plotted in the GaussView5.0 molecular imaging software [35], the initial geometries of the molecules were obtained using the GaussView 5.0 packet software to and calculated in the Gaussian09W software [36, 37] (Fig. 1). In order to better determination of the electronic properties of the structures, the DFT method is used which takes into account the electron density and produces the desired data over this electron density. B3LYP is popular for many reasons. It was one of the first DFT methods that was a significant improvement over Hartree-Fock. B3LYP is generally faster than most Post Hartree-Fock techniques and usually yields comparable results. It is also fairly robust for a DFT method. On a more fundamental level, it is not as heavily parameterized as other hybrid functionals [38]. In addition, the hybrid function B3LYP in the Gaussian09W software, which is suitable for the workstation's capacity and 6-31G(d,p) [38] as the basic set were used. All calculations were made on computers located in Chemistry Department of Kafkas University Science Faculty.

Electronic structure identifiers from all the geometry-optimized structures and E_{HOMO}, E_{LUMO}, ΔE, η, σ, χ, nucleophilicity (ε) index, electrophilicity (ω) index, chemical potential (Pi), μ and the ΔN associated with corrosion inhibition activity were calculated. In addition to the electronic structure identifiers, the total negative charge (TNC) parameter is also investigated.

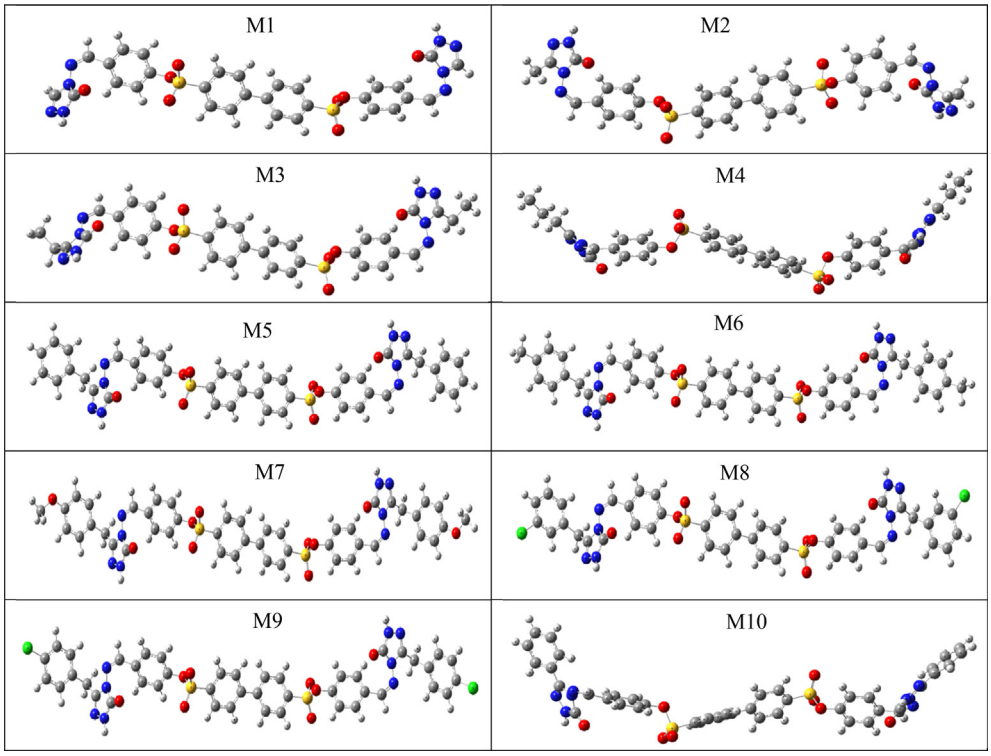

Fig. 1. The optimized gas-phase molecules at DFT/B3LYP theoretical level using 6-31G(d,p) basis set.

3. Results and discussion

3.1. Experimental analysis

When IR spectral data of the {bis-4-[(3-alkyl-5-oxo-1H-1,2,4-triazol-4(5H)-yl)-iminomethyl]-phenyl} [1,1′-biphenyl]-4,4′-disulfonate compounds **(M2-10)** are examined, it have seen that there are N-H stretching vibrations in the range of 3212-3170 cm^{-1} and carbonyl (C=O) peak in the range of 1739-1694 cm^{-1}. It have been found that these results are compatible with the structure. In ^{1}H-NMR spectra of the compounds, The peaks of the N-H protons were observed in the range of 12.41-11.85 ppm. The protons of azomethine moiety (N=CH) were found at δ 9.71–9.64 ppm. Theese data are consistent with the literature. Aromatic protons of 1,4-disubstituted benzene ring in the range of δ 8.10–6.83 ppm and aromatic protons bound to C-3 in the triazole ring were found to be consistent with the values given in the literature. Additionally, When ^{13}C-NMR spectra were examined, it have been observed 1,2,4-triazole C-5 carbons in the range of the δ 154.85–151.73 ppm, azomethine carbons (N=CH) in the range of the δ 151.28–151.06 ppm and triazole C-3 carbons in the range of the 148.04–144.26 ppm. Also, differentiation of aromatic carbons of aryl groups in {bis-4-[(3-alkyl-5-oxo-1H-1,2,4-triazol-4(5H)-yl)-iminomethyl]-phenyl} [1,1′-biphenyl]-4,4′-disulfonate compounds have been achieved. Aromatic carbon and aromatic hydrogen data bonded to the C-3 in the triazole ring were determined as underlined.

3.2. Geometry optimization

Gas phase geometry optimizations of all the structures (**M1-10**) (Fig. 1) studied were primarily determined by using the MM2 method and followed by the subsequent semi empirical PM3 consistent molecular orbital (SCFMO) method. Advanced geometry optimizations were achieved using RHF and B3LYP/6-31G(d,p) base sets. Normal mode analysis for each structure did not result in any negative frequencies in all three calculation methods [39].

3.3. Inhibitor activity parameters

Identifiers derived from the electronic structure of the molecule, which are linked to the electronic structure, are called electronic structure identifiers [40]. Some of them are, the E_{HOMO}, E_{LUMO}, ΔE_{gap}, η, σ, χ, Pi, ω, ε and μ. Among these identifiers, HOMO, LUMO and μ are obtained from the Gaussian output file of the molecule. Other identifiers can be calculated by existing equations in the literature.

According to the Koopman's theorem, E_{HOMO} and E_{LUMO} values of any chemical type are associated with its ionization energy and electron affinity values [40, 41]. ΔE [42], η [43], σ [44], χ and Pi [45] can be calculated by the following.

$$I = -E_{HOMO} \text{ [40, 41]} \quad (1)$$

$$A = -E_{LUMO} \text{ [40, 41]} \quad (2)$$

$$\Delta E = (E_{LUMO} - E_{HOMO}) \text{ [42]} \quad (3)$$

$$\eta = (I - A) / 2 \text{ [43]} \quad (4)$$

$$\sigma = 1/\eta \text{ [44]} \quad (5)$$

$$\chi = (I + A) / 2 \text{ [45]} \quad (6)$$

$$P_i = -\chi \text{ [45]} \quad (7)$$

The electrophilicity (ω) index is a measure of the energy depletion due to the maximum electron flow between the transmitter and the receiver [46]. The equation is given as it is in 8. The nucleophilicity (ε) index is a new molecular structure identifier [47]. The equation is given as it is in 9.

$$\omega = P_i^2/2\eta \text{ [46]} \quad (8)$$

$$\varepsilon = P_i \,.\, \eta \text{ [47]} \quad (9)$$

ΔN of the electrons transferred between the inhibitor and the metal is calculated by the following equation using the theoretically calculated χ and η values [48]. The $\chi_{inhibitor}$ and $\eta_{inhibitor}$ values of the inhibitor in the equation are calculated theoretically while the χ_{metal} and η_{metal} values of the metal atom are experimentally determined by Pearson. According to Pearson, since the electron affinity (A) and the ionization potential (I) of a single metal is assumed equal (I = A), the η_{metal} value is taken as zero for a single metal [47]. The total energy, TNC [49, 50] and electron structure identifiers of all the molecules studied are given in Table 2.

$$\Delta N = (\chi_{metal} - \chi_{inhibitor}) / 2.(\eta_{metal} - \eta_{inhibitor}) \text{ [48]} \quad (10)$$

When we look at the HOMO and LUMO energies in Table 2 of the studied constructions, it seems that there is a general tendency among them. E_{HOMO} order is as shown below.

M7 > M10 > M6 > M4 > M5 > M9 = M8 > M1 > M2 > M3

Since HOMO is related to electron donating capacity, it is important for corrosion studies. It can be said that the inhibitory effect of inhibitor molecules increases with increasing HOMO values [51]. Thus it acts on the charge transfer mechanism along the metal surface, enabling adsorption. It is seen that compound **M7** having the highest inhibitory activity and compound **M3** having the lowest inhibitory activity are seen to have the highest inhibitory activity according to the high E_{HOMO} value (Fig. 2).

LUMO is about the ability to accept electrons. Low valued E_{LUMO} indicates that the inhibitor can place an additional negative charge on the metal surface. E_{LUMO} order is as shown below.

M7 > M5 > M6 > M4 > M10 > M1 > M9 = M8 > M2 > M3

The E_{LUMO} sequence shows that LUMO energy of **M3** has the lowest energy and the LUMO energy of **M7** is with the highest energy. LUMO energy values of inhibitors with high HOMO energy values were also found to be high. For this reason, it was determined that the **M7** inhibitor was reactive by acting as a donor and accordingly its inhibitor activity was high. The lowest E_{LUMO} and the lowest E_{HOMO} values belong to the **M3** inhibitor. While inhibitors with low E_{HOMO} reduce the reactivity to metal, the metal inhibitor acts as a donor to the inhibitor. Accordingly, the activity of the inhibitor is reduced while the reactivity of the metal is increased. According to HOMO-LUMO energies, **M7** molecule has the most effective corrosion inhibition (Fig. 2).

The energy gap between E_{HOMO} and E_{LUMO} has a very large preliminary significance and clarity in order to determine the theoretical inhibition efficiency, as well as the static molecular reactivity. According to the energy gap value, the sequence of the inhibitors is as follows:

M1 > M8 = M9 > M5 > M4 > M6 > M10 > **M7** > M2 > M3

The energy gap is a measure of another molecule's activity against the molecule. It is important to compare ΔE for inhibitor studies. The lower the absolute value of the energy gap, the better efficiency of inhibition. The lower value of ΔE in corrosion inhibitors depends on the E_{HOMO} rather than the E_{LUMO}. Inhibitor derivatives with high HOMO energy and low ΔE can be used as good anti-corrosion agents [51]. Given the above E_{HOMO} and ΔE sequence, it can be said that **M7** will provide a good inhibition activity depending on the highest value of HOMO energy.

It is also supported by the TNC values [49, 50] that **M7** has the most effective corrosion inhibition. The TNC is about the ability to become an electron donor. From the TNC values in Table 2, it is seen that the most negative load is in the **M7** inhibitor. The fact that the number of heteroatoms in the **M7** inhibitor is high plays an important role in this. Unlike other molecules at **M7**, oxygen atoms in the substituent position increase TNC [49, 50]. In addition, the HOMO in the orbital diagram in Fig. 2 supports this situation in centers.

Charges of the atoms in the molecular structure of the **M7** inhibitor is shown in Table 3. The use of Mulliken population analysis is a widely used method for predicting the adsorption centers of the inhibitor molecules [51] (Table 3). It has been supported by many researchers that the

Table 2
Total energy, sum of negative charges (TNC) and values of electron structure identifiers calculated using 6–31g(d,p) basis set at the DFT/B3LYP theory level of molecules in gas phase.

Molecule Name	Total Energy (a.u)	μ (D)	E_{HOMO} (eV)	E_{LUMO} (eV)	ΔE (eV)	χ (eV)	η (eV)	σ (eV^{-})	Pi (eV)	ω (eV)	ε (eV)	ΔN	TNC (a.u)
M1	-2992.377	2.4448	-6.16	-2.34	3.82	4.25	1.910	0.52	-4.25	4.73	-8.12	0.7198	-9.8673
M2	-3070.042	4.2033	-6.19	-3.44	2.75	4.82	1.375	0.73	-4.82	8.43	-6.63	0.7899	-7.3051
M3	-3149.272	4.1536	-6.40	-3.82	2.58	5.11	1.290	0.78	-5.11	10.12	-6.59	0.7325	-11.3425
M4	-3228.283	3.4871	-5.98	-2.32	3.66	4.15	1.830	0.55	-4.15	4.71	-7.59	0.7787	-12.2363
M5	-3533.123	2.9624	-6.00	-2,31	3.69	4.16	1.845	0.54	-4.16	4.68	-7.68	0.7710	-11.4255
M6	-3611.759	2.7760	-5.96	-2.31	3.65	4.14	1.829	0.55	-4.14	4.67	-7.57	0.7836	-13.4535
M7	-3762.169	2.4405	-5.77	-2.30	3.47	4.04	1.735	0.58	-4.04	4.69	-7.01	0.8546	-13.8930
M8	-4452.315	4.2006	-6.12	-2.37	3.75	4.25	1.875	0.53	-4.25	4.81	-7.97	0.7333	-12.3571
M9	-4452.315	4.6612	-6.12	-2.37	3.75	4.25	1.875	0.53	-4.25	4.81	-7.97	0.7333	-12.3448
M10	-3454.500	3.8228	-5.86	-2.33	3.53	4.09	1.765	0.57	-4.09	4.75	-7.22	0.8229	-11.6587

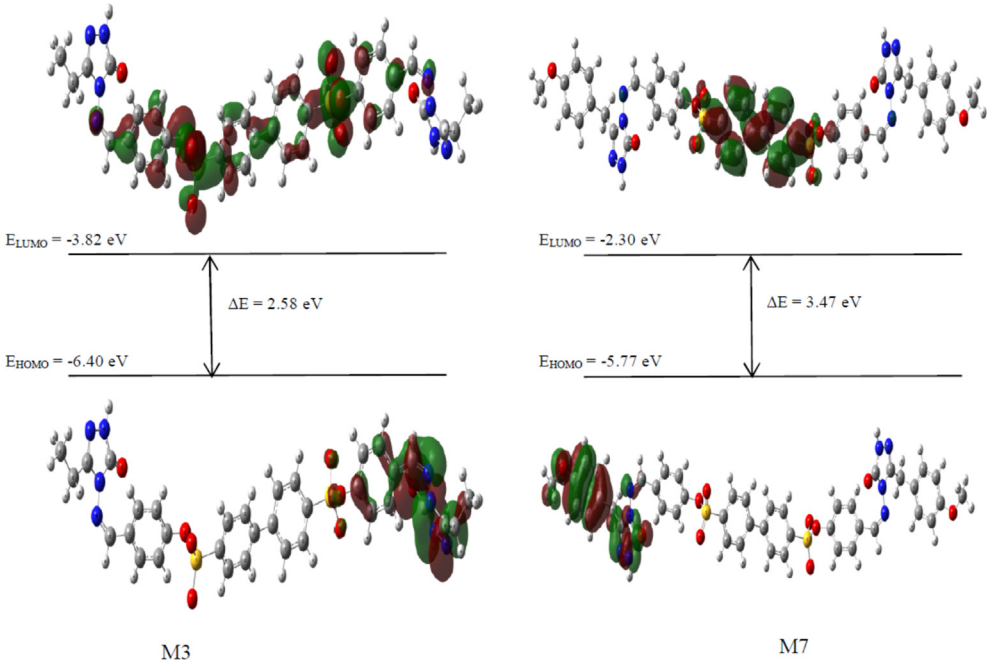

Fig. 2. HOMO-LUMO energy diagrams of M3 and M7 inhibitors.

presence of negatively charged heteroatoms increases the ability to adsorb on the metal surface by donor-acceptor mechanism [52]. In view of this information, **M7** has an effective inhibitory effect due to negatively charged nitrogen atoms, oxygen atoms and carbons in the aromatic ring. Looking at the MEP map in Fig. 3, it is seen that the oxygen bound to the triazole ring has a denser red color than the other negative atoms. This can be interpreted as the fact that the **M7** inhibitor can be coordinately bound to the metal surface, again from these centers.

η and σ are other important parameters that give information about the stability, reactivity and inhibitor activity of an inhibitor. The η and σ of the grading of said inhibitors should be as follows, respectively:

M1 > M9 = M8 > M5 > M4 ≈ M6 > M10 > **M7** > M2 > M3

M3 > M2 > **M 7** > M10 > M4 ≈ M6 > M5 > M9 = M8 > M1

Since the organic selected as an inhibitor behaves as a lewis base, and soft inhibitors are more reactive compared to hard inhibitors, they behave as better corrosion inhibitors [53, 54, 55]. In this case it was calculated that the **M7** inhibitor with high E_{HOMO} and low ΔE had high softness and low hardness values. The η and σ values support that the M7 inhibitor has the most effective inhibitory effect.

χ and Pi are other parameters that are calculated for inhibitor activity. The sequence of χ is as follows:

M3 > M2 > M1 ≈ M9 = M8 > M5 > M4 > M6 > M10 > **M7**

The calculated χ values of the inhibitors give information on how the coordinated covalent bond between the metal and the inhibitor occurs [51]. In this study, corrosion inhibition activity of the molecules designed as inhibitors on iron metal was examined. The χ values of the inhibitors calculated in Table 2 were found to be lower than the experimental χ value of the iron metal. Thus, it has been determined that the iron metal will form bonds by taking electrons from the inhibitor compound. When we look at the χ sequence, the **M7** inhibitor will act as the most effective corrosion inhibitor with the lowest χ value. Pi the inverse of electronegativity. That is, a molecule with a high chemical potential has a high activity against other molecules, while a molecule with a low potential has low activity against other molecules [56]. As shown in Table 2, the inhibitor with the highest activity is **M7**.

When look at the ΔN [48] values obtained for iron and metal inhibitors (Table 2), it can be said that **M7** molecule transfers more electrons to the iron metal, thus it is a more effective inhibitor.

Another parameter shown in Table 2 is the dipole moment. However, studies in the literature have not found a clear link between μ and inhibition activity. In some studies, it is said that the activity of molecules with higher μ value leads to better inhibition, while in other studies it is said that the inhibition effect increases with decreasing μ value. The **M7** inhibitor, which is in compliance with other parameters, has low dipole moment. This can be interpreted as a better covering of the metal surface at low μ values.

ω and ε indices are important parameters used in the activities of corrosion inhibitors. The ω index indicates the ability of inhibitor

Table 3
Mulliken charges of atoms in the molecule structure of the M7 inhibitor.

C1	0.561614	**H27**	0.18691	**C53**	0.206151	**H79**	0.141365
C2	0.772269	**C28**	-0.1671	**H54**	0.149232	**C80**	-0.17367
N3	-0.44505	**H29**	0.187197	**H55**	0.157271	**H81**	0.128836
H4	0.354664	**C30**	0.093265	**C56**	-0.00027	**C82**	0.375531
N5	-0.33064	**H31**	0.154941	**H57**	0.160913	**H83**	0.131456
N6	-0.4997	**H32**	0.155615	**N58**	-0.44543	**C84**	0.172882
N7	-0.24602	**O33**	-0.50899	**C59**	0.771182	**C85**	-0.18769
O8	-0.52342	**O34**	-0.50984	**C60**	0.56116	**C86**	-0.17472
C9	-0.0008	**C35**	0.092915	**H61**	0.355246	**C87**	-0.193
H10	0.162424	**C36**	-0.1674	**N62**	-0.33084	**H88**	0.141191
C11	0.204875	**C37**	-0.1677	**N63**	-0.49992	**C89**	-0.17371
C12	-0.16703	**C38**	-0.13745	**O64**	-0.51866	**H90**	0.12947
C13	-0.20095	**H39**	0.155018	**S65**	1.247116	**C91**	0.375342
C14	-0.12984	**C40**	-0.13436	**O66**	-0.51184	**H92**	0.131282
H15	0.1579	**H41**	0.155337	**O67**	-0.49603	**H93**	0.136945
C16	-0.12918	**C42**	-0.15563	**N68**	-0.24794	**O94**	-0.50708
H17	0.148353	**H43**	0.189324	**C69**	-0.42547	**C95**	-0.21458
C18	0.319673	**H44**	0.186947	**H70**	0.181434	**H96**	0.152393
H19	0.16181	**O45**	-0.6141	**H71**	0.166637	**H97**	0.169217
H20	0.160349	**C46**	0.326608	**C72**	-0.42526	**H98**	0.151105
O21	-0.61277	**C47**	-0.13817	**H73**	0.1821	**H99**	0.136678
S22	1.24922	**C48**	-0.14162	**H74**	0.168169	**O100**	-0.50723
C23	-0.1564	**C49**	-0.20212	**C75**	0.172655	**C101**	-0.21463
C24	-0.13485	**H50**	0.176131	**C76**	-0.18754	**H102**	0.152794
C25	-0.1355	**C51**	-0.16623	**C77**	-0.17407	**H103**	0.169194
C26	-0.16761	**H52**	0.153749	**C78**	-0.19303	**H104**	0.150984

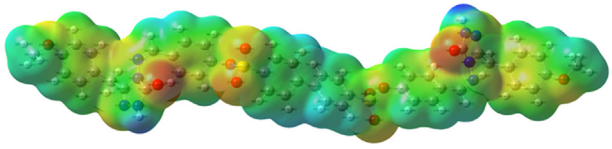

Fig. 3. MEP map of M7 inhibitor.

molecules to accept electrons [46]. The ε index shows the ability of the inhibitors to donate electrons [57]. The inhibition activity increases with decreasing ω value or increasing ε value [58]. According to ω and ε, the theoretical inhibition efficiency sequence is as follows:

M3 > M2 > M9 = M8 > M10 > M1 > M4 > **M7** > M5 > M6

M3 > M2 > **M7** > M10 > M6 > M4 > M5 > M9 = M8 > M1

As can be seen in the sequence, the calculated ω value of the **M7** inhibitor decreased, and the ε value increased. It is observed that the **M7** inhibitor has the most effective inhibitory effect with ω and ε values in accordance with other parameters.

4. Conclusion

In this study, the structures of nine new {Bis-4-[3-(alkyl-5-oxo-1H-1,2,4-triazol-4(5H)-yl)-iminomethyl]-phenyl} [1,1′-biphenyl]-4,4′-disulfonate (M2-10) synthesized from the reactions of **T** type compounds with bis-(4-formylphenyl) [1,1′-biphenyl]-4,4′-disulfonate **(A)** were identified using IR, ^{1}H NMR and ^{13}C NMR spectral data.

According to the obtained results, E_{LUMO} values of inhibitors with high E_{HOMO} values were also found to be high. For this reason, it was determined that the **M7** inhibitor was reactive by acting as a donor and accordingly its inhibitor activity was high. Inhibitor derivatives with high E_{HOMO} and low ΔE can be used as good anti-corrosion agents. Given the E_{HOMO} and ΔE sequence, it can be said that compound **M7** will provide a good inhibition activity depending on the highest value of E_{HOMO}. It can be interpreted as the fact that the **M7** inhibitor, which is included in the study, is better at covering the metal surface at low dipole moment value, although a clear conclusion about the dipole moment is not found in the literature.

When look at the Mulliken atomic charges of the **M7** inhibitor, it can be said that the electronegative atoms have a great effect on the inhibition activity, the negatively charged atoms have HOMO centers on them, and from there the inhibitor can be bound to the metal surface from these centers. The TNC value associated with the ability to donate is highest in the **M7** molecule. It has been seen that the most active region in the MEP map is around the oxygen(s) bound to the triazole(s) (Fig. 3).

The calculated η, σ, χ, Pi, ω and ε parameters support that the **M7** inhibitor has the most effective corrosion inhibition effect. The lower χ value of the inhibitor shows that the iron metal will form a bond by taking electrons from the inhibitor compound and the higher ΔN value of the inhibitor shows that it will be better adsorbed to the metal surface and the corrosion inhibition effect will increase.

It is revealed that there is a close relationship between the activity of organic-based corrosion inhibitors showing good corrosion inhibitor activity and the calculated quantum chemical parameters of the process. One of its greatest advantages is that the studied structure can be changed in accordance with calculations.

The **M7** compound has effective corrosion inhibition properties and is thought to exhibit more effective inhibitor properties, if the number of heteroatoms in the structures of other molecules is increased.

Declarations

Author contribution statement

Murat Beytur: Conceived and designed the experiments; Performed the experiments; Analyzed and interpreted the data; Contributed reagents, materials, analysis tools or data; Wrote the paper.

Zeynep T. Irak: Conceived and designed the experiments; Analyzed and interpreted the data; Contributed reagents, materials, analysis tools or data; Wrote the paper.

Sevda Manap, Haydar Yüksek: Conceived and designed the experiments; Performed the experiments; Analyzed and interpreted the data.

Funding statement

This work was supported by the Scientific Research Projects Coordination Unit of Kafkas University (Project Number: 2016-FM-09).

Competing interest statement

The authors declare no conflict of interest.

Additional information

No additional information is available for this paper.

References

[1] H. Schiff, Mitteilungen aus dem universitatslaboratorium in Pisa: Eineneue reihe organischer basen (in German), Ann. Chem. 131 (1864) 118–119.
[2] C.M. Silva, D.N. Silva, L.V. Modolo, R.B. Alves, M.A. Resende, C.V.B. Martins, A. Fatima, Schiff bases: a short review of their antimicrobial activities, Cario Univ. J. Adv. Res. (2011) 1–8.
[3] K. Brodowska, E. Ludyga-Chruscinska, Schiff bases-interesting range of applications in various field of science, CHEMIK 68 (2014) 129–134.
[4] A. Prakash, D. Adhikari, Application of Schiff bases and their metal complexesa review, Int. J. Chem. Tech. Res. 3 (2011) 1891–1896.
[5] W.A. Zopubi, Biological activities of Schiff bases and their complexes: a review of recent work, Int. J. Org. Chem. 3 (2013) 73–95.
[6] K.C. Gupta, A.K. Sutar, Catalytic activities of Schiff base transition metal complexes, Coord. Chem. Rev. 252 (2008) 1420–1450.
[7] W. Qin, S. Long, M. Panunzio, S. Biondi, Schiff bases: a short survey on an evergreen chemistry tool, Molecular 18 (2013) 12264–12289.
[8] S. Park, V.K. Mathur, R.P. Planalp, Syntheses, solubilities and oxygen absorption properties of new cobalt (II) Schiff-base complexes, Polyhedron 17 (2–3) (1998) 325–330.
[9] X. Lu, S.Y. Qin, Z.Y. Zhou, V. Yam, Synthesis, structure, and ion-binding studies of cobalt (II) complexes with aza-crown substituted salicylaldimine Schiff base ligand, Inorg. Chim. Acta 346 (2003) 49–56.
[10] G.H. Olive, S. Olive, The Chemistry of the Catalyzed Hydrogenation of Carbon Monoxide, Springer Science & Business Media, 2012.
[11] S.H. Rahaman, H. Choowdhury, D. Bose, R. Ghosh, G. Chen-Hsing, K. Barindra, H. Ghosh, Synthesis, structure and properties of mononuclear cobalt (II) and cobalt (III) pseudohalide complexes containing N-donor Schiff bases: synthetic control of metal oxidation levels, Polyhedron 24 (13) (2005) 1755–1763.
[12] H. Kunkely, A. Vogler, Photochemistry of N, N′-bis (3, 5-di-tert-butylsalicylidene)-1, 2-diaminocyclohexane and its Co (II) complex in chloroform, J. Photochem. Photobiol. A Chem. 138 (1) (2001) 51–54.
[13] A. Mederos, S. Domínguez, R. Hernández-Molina, J. Sanchiz, F. Brito, Coordinating ability of ligands derived from phenylenediamines, Coord. Chem. Rev. 193 (1999) 857–911.
[14] N. Gumrukcuoglu, Z. Bahadır, M. Ocak, U. Ocak, Determination of stability constants of triazole ligand carrying naphthol group with heavy metal ions in aqueous solutions, Pak. J. Anal. Environ. Chem. 14 (2) (2013) 7.
[15] S. Deng, X. Li, H. Fu, Two pyrazine derivatives as inhibitors of thecold rolled steel corrosion in hydrochloric acid solution, Corros. Sci. 53 (2011) 822–828.
[16] A.S. Patel, V.A. Panchal, G.V. Mudaliar, N.K. Shah, Impedance spectroscopic study of corrosion inhibition of Al-pure by organic schiff base in hydrochloric acid, King Saud University, J. Saudi Chem. Soc. (2013).
[17] X. Li, S. Deng, H. Fu, Three pyrazine derivatives as corrosion inhibitors for steel in 1.0 M H2SO4 solution, Corros. Sci. 53 (10) (2011) 3241–3247.
[18] M. Karelson, V.S. Lobanov, A.R. Katritzky, Quantum-chemical descriptors in QSAR/QSPR studies, Chem. Rev. 96 (3) (1996) 1027–1044.
[19] J. Fang, J. Li, Quantum chemistry study on the relationship between molecular structure and corrosion inhibition efficiency of amides, J. Mol. Struct. 593 (2002) 179–185.
[20] F. Kandemirli, S. Sağdinç, Theoritical study of corrosion ınhibition of amides and thiosemicarbazones, Corros. Sci. 49 (2007) 2118–2130.
[21] A. Yurt, G. Bereket, C. Ogretir, Quantum chemical studies on inhibition effect of amino acids and hydroxy carboxylic acids on pitting corrosion of aluminium alloy 7075 in NaCl solution, J. Mol. Struct. 725 (1-3) (2005) 215–221.
[22] S. Chen, Z. Liu, H. Ma, Y. Sun, Theoretical elucidation on the inhibition mechanism of pyridine–pyrazole compound: a Hartree Fock study, J. Mol. Struct. 774 (2006) 19–22.
[23] T. Arslan, F. Kandemirli, E.E. Ebenso, I. Love, H. Alemu, Quantum chemical studies on the corrosion inhibition of some sulphonamides on mild steel in acidic medium, Corros. Sci. 51 (2009) 35–47.
[24] W. Kohn, L.J. Sham, Self-consistent equations including exchange and correlation effects, Phys. Rev. 140 (4A) (1965) A1133.
[25] R.G. Parr, W. Yang, Density-functional Theory of Atoms and Molecules, 1989, p. 333.
[26] L.J. Bartolotti, K. Flurchick, An introduction to density functional theory, Rev. Comput. Chem. 7 (1996) 187–260.
[27] L.M. Rodriguez-Valdez, A. Martinez-Villafane, D. Glossman-Mitnik, CHIH-DFT determination of the molecular structure, infrared and ultraviolet spectra of potentially organic corrosion inhibitors, J. Mol. Struct. 681 (2004) 83–88.
[28] W. Li, Q. He, C. Pei, B. Hou, Experimental and theoretical investigation of the adsorption behaviour of new triazole derivatives as inhibitors of mild steel corrosion in acid media, Electrochim. Acta 52 (2007) 6386–6394.
[29] F. Bentiss, M. Traisnel, N. Chaibi, B. Mernari, H. Vezin, M. Lagrenée, 2,5-Bis(n methoxyphenyl)-1,3,4 oxadiazoles used as corrosion inhibitors in acidic media: correlation between inhibition efficiency and chemical structure, Corros. Sci. 44 (2002) 2271–2289.
[30] M. Özcan, I. Dehri, M. Erbil, Organic sulphur-containing compounds as corrosion inhibitors for mild steel in acidic media: correlation between inhibition efficiency and chemical structure, Appl. Surf. Sci. 236 (2004) 155–164.
[31] R. Hasanov, M. Sadıkoglu, S. Bilgiç, Electrochemical and quantum chemical studies of some Schiff bases on the corrosion of steel in H2SO4 solution, Appl. Surf. Sci. 253 (2007) 3913–3921.
[32] H. Ju, Z.P. Kai, Y. Li, Aminic nitrogen-bearing polydentate Schiff base compounds as corrosion inhibitors for iron in acidic media: a quantum chemical calculation, Corros. Sci. 50 (2008) 865–871.
[33] G. Gece, The use of quantum chemical methods in corrosion inhibitor studies, Corros. Sci. 50 (2008) 2981–2992.
[34] A.A. Ikizler, R. Ün, Reactions of ester ethoxycarbonylhydrazones with some amine type compounds, Chim. Acta Turc. 7 (1979) 269–290.
[35] R. Dennington, T. Keith, J. Millam, GaussView, Version 5, Semichem Inc., Shawnee Mission KS, 2009.
[36] M.J. Frisch, G.W. Trucks, H.B. Schlegel, G.E. Scuseria, M.A. Robb, J.R. Cheeseman, G. Scalmani, V. Barone, B. Mennucci, G.A. Petersson, H. Nakatsuji, M. Caricato, X. Li, H.P. Hratchian, A.F. Izmaylov, J. Bloino, G. Zheng, J.L. Sonnenberg, M. Hada, M. Ehara, K. Toyota, R. Fukuda, J. Hasegawa, M. Ishida, T. Nakajima, Y. Honda, O. Kitao, H. Nakai, T. Vreven, J.A. Montgomery, T. Vreven Jr., J.E. Peralta, F. Ogliaro, M. Bearpark, J.J. Heyd, E. Brothers, N. Kudin, V.N. Staroverov, R. Kobayashi, J. Normand, K. Raghavachari, A. Rendell, J.C. Burant, S.S. Iyengar, J. Tomasi, M. Cossi, N. Rega, J.M. Millam, M. Klene, J.E. Knox, J.B. Cross, V. Bakken, C. Adamo, J. Jaramillo, R. Gomperts, R.E. Stratmann, O. Yazyev, A.J. Austin, R. Cammi, C.J. Pomelli, W. Ochterski, L.R. Martin, K. Morokuma, V.G. Zakrzewski, G.A. Voth, P. Salvador, J.J. Dannenberg, S. Dapprich, A.D. Daniels, O. Farkas, J.B. Foresman, J.V. Ortiz, J. Cioslowski, D.J. Fox, Gaussian Inc., 2009. Wallingford, CT.
[37] J.B. Foresman, Æ. Frisch, Exploring Chemistry with Electronic Structure Methods, second ed., vol. 266, Gaussian Inc, Pittsburgh, PA, 1996, pp. 278–283.
[38] A.D. Becke, Density-functional thermochemistry. IV. A new dynamical correlation functional and implications for exact-exchange mixing, J. Chem. Phys. 104 (3) (1996) 1040–1046.
[39] Z. Turhan Irak, S. Gümüş, Heterotricyclic compounds via click reaction: a computational study, Noble Int. J. Sci. Res. 1 (7) (2017) 80–89.
[40] T. Koopmans, Über die zuordnung von wellenfunktionen und eigenwerten zu den einzelnen elektronen eines atoms, Physica (Amsterdam) 1 (1933) 104.
[41] B.N. Plakhutin, E.R. Davidson, Koopmans' theorem in the restricted open-shell Hartree−Fock method. 1. A variational approach, J. Phys. Chem. A 113 (45) (2009) 12386–12395.
[42] E. Jesudason, S.K. Sridhar, E.J. Malar, P. Shanmugapandiyan, M. Inayathullah, V. Arul, D. Selvaraj, R. Jayakumar Synthesis, Pharmacological screening, quantum chemical and in vitro permeability studies of N-Mannich bases of benzimidazoles through bovine cornea, Eur. J. Med. Chem. 44 (2009) 2307–2312.
[43] H. Gökçe, S. Bahçeli, A study on quantum chemical calculations of 3-, 4-nitrobenzaldehyde oximes, Spectrochim. Acta A. 79 (2011) 1783–1793.
[44] M. Arivazhagan, V.P. Subhasini, Quantum chemical studies on structure of 2-amino-5-nitropyrimidine, Spectrochim. Acta 91 (2012) 402–410.
[45] M.S. Masoud, A.E. Ali, M.A. Shaker, G.S. Elasala, Synthesis, computational, spectroscopic, thermal and antimicrobial activity studies on some metal–urate complexes, Spectrochim. Acta A 90 (2012) 93–108.
[46] S. Kiyooka, D. Kaneno, R. Fujiyama, Parr's index to describe both electrophilicity and nucleophilicity, Tetrahedron Lett. 54 (2013) 339.
[47] R.G. Pearson, Absolute electronegativity and hardness: application to inorganic chemistry, Inorg. Chem. 27 (1987) 734–740.
[48] A.Y. Musa, R.T.T. Jalgham, A.B. Mohamad, Molecular dynamic and quantum chemical calculations for phthalazine derivatives as corrosion inhibitors of mild steel in 1 M HCl, Corros. Sci. 56 (2012) 176–183.
[49] G. Bereket, C. Ogretir, C. Ozsahin, Quantum chemical studies on the inhibition efficiencies of some piperazine derivatives for the corrosion of steel in acidic medium, J. Mol. Struct. 663 (2003) 39–46.
[50] R.M. Issa, M.K. Awad, F.M. Atlam, Quantum chemical studies on the inhibition of corrosion of copper surface by substituted uracils, Appl. Surf. Sci. 255 (2008) 2433–2441.
[51] S. Chen, B. He, Y. Liu, Y. Wang, J. Zhu, Quantum chemical study of some benzimidazole and its derivatives as corrosion ınhibitors of steel in HCl solution, Int. J. Electrochem. Sci. 9 (2014) 5400–5408.
[52] Z. El Adnani, M. Mcharfi, M. Sfaira, M. Benzakour, A.T. Benjelloun, M. Ebn Touhami, DFT theoretical study of 7-R-3-methylquinoxalin-2(1H)-thiones (R=H; CH3; Cl) as corrosion inhibitors in hydrochloric acid, Corros. Sci. 68 (2013) 223–230.
[53] E. Fujioka, H. Nishihara, K. Aramaki, The inhibition of pit nucleation and growth on the passive surface of iron in a borate buffer solution containing Cl by oxidizing inhibitors, Corros. Sci. 38 (1996) 1915–1933.
[54] E.C. Koch, Acid–base interactions in energetic materials: I. The hard and soft acids and bases (HSAB) principle–insights to reactivity and sensitivity of energetic materials, Propell. Explos. Pyrotech. 30 (2005) 5–16.
[55] D.B. Alexander, A.A. Moccari, Evaluation of corrosion inhibitors for component cooling water systems, Corrosion 49 (1993) 921–928.
[56] S. Kaya, S. Erkan Kariper, A. Ungördü, C. Kaya, Effect of some electron donor and electron acceptor groups on stability of complexes according to the principle of HSAB, J. N. Results Sci. 4 (2014) 82–89.
[57] S. Erkan Kariper, K. Sayın, D. Karakas, Theoretical studies on eight oxovanadium(IV) complexes with salicylaldehyde and aniline ligands, Hacet. J. Biol. Chem. 42 (3) (2014) 337–342.
[58] N. Karakus, K. Sayin, The investigation of corrosion inhibition efficiency on some benzaldehyde thiosemicarbazones and their thiole tautomers: computational study, J. Taiwan Inst. Chem. Eng. 48 (2015) 95–102.